Int. J. Multiphase Flow Vol. 12, No. 1, pp. 79–98, 1986
Printed in Great Britain.

0301–9322/86 \$3.00 + .00
Pergamon/Elsevier

PREDICTION OF THE INITIATION OF SLUGS WITH LINEAR STABILITY THEORY

P. Y. LIN and T. J. HANRATTY
Department of Chemical Engineering, University of Illinois, Urbana, IL 61801, U.S.A.

(*Received* 20 *August* 1984; *in revised form* 16 *May* 1985)

Abstract—This paper explores the application of linear stability theory to explain the onset of slugging. It is shown that the inviscid Kelvin–Helmholtz theory correctly predicts stability of a stratified flow only for very large liquid viscosities. In general, however, inviscid theory is in error because it ignores the destabilizing effect of liquid inertia. Good agreement is noted between the linear stability analysis and observations of the initiation of slugs in 2.54- and 9.53-cm horizontal pipes at superficial gas velocities less than 3.3 m/s.

1. INTRODUCTION

A transition from a stratified to a slug pattern in horizontal concurrent gas–liquid flow happens when a disturbance at the gas–liquid interface, which grows rapidly to block the cross-section of the conduit, is propelled violently downstream as a slug. The occurrence is of concern to the process industry since slugs cause oscillations in the flow rate and in the pressure, which can severely damage equipment. This paper explores the application of linear stability theory to explain the onset of slugging for flow in a rectangular channel and in a pipe, and uses it to examine the effects of liquid viscosity and conduit size on the instability.

Theoretical predictions for the onset of slugging have been presented by a number of investigators, who applied classical Kelvin–Helmholtz instability theory to ideal inviscid fluids. Slugs are pictured to form when the suction pressure generated over a wave by the Bernoulli effect is large enough to overcome the stabilizing influence of gravity.

The use of inviscid Kelvin–Helmholtz instability theory implies that liquid inertia terms do not contribute to the instability, that forces causing instability are in phase with the wave height, and that shear stress terms are unimportant.

For flow in a channel of height B, inviscid theory predicts the growth of infinitesimal long wavelength disturbances, provided the following relation holds:

$$\frac{V_{SG}}{\sqrt{gB}}\sqrt{\frac{\rho_G}{\rho_L-\rho_G}} \geq \alpha^{3/2}, \qquad [1]$$

where V_{SG} is the superficial gas velocity and α, the void fraction, and ρ_G, ρ_L, the densities of the gas and liquid phases.

Wallis & Dobson (1973) performed transition studies in rectangular channels and concluded that [1] overpredicts the critical gas velocity by a factor of about two. They explained their data by extending Benjamin's (1968) work for liquid flow around a stagnant bubble to gas flow around a stagnant slug. This theory has not been widely accepted.

In an earlier work, Kordyban & Ranov (1970) extended classical Kelvin–Helmholtz theory to finite amplitude waves in inviscid flow and obtained an instability criterion for channel flow. In order to evaluate this criterion, however, the wave number must be known and a relationship between wave amplitude and wave length formulated. Kordyban (1977), more recently, applied the inviscid Kelvin–Helmholtz stability just to the crest of an existing wave. The instability criterion is given as

$$\frac{V_C^2}{gh_G}\left(\frac{\rho_G}{\rho_L-\rho_G}\right)=\frac{1}{K_1}, \qquad [2]$$

where K_1 was determined from experiments to be 1.35.

Taitel & Dukler (1976) applied the Kelvin–Helmholtz instability mechanism to a solitary wave of finite amplitude in pipe flow and arrived at the criterion

$$F=\frac{V_{SG}}{\sqrt{gD}}\sqrt{\frac{\rho_G}{\rho_L-\rho_G}}\geq K_2 f\left(\frac{h}{D}\right), \qquad [3]$$

where h is the height of the liquid and D the pipe diameter. Using qualitative arguments, they speculate that K_2 can be estimated as

$$K_2=1-h/D. \qquad [4]$$

Even though Taitel & Dukler included viscous terms to evaluate h/D in their analysis of equilibrium stratified flow, the instability criterion, itself, was derived using inviscid fluid theory.

Mishima & Ishii (1980) reexamined the analysis of Kordyban & Ranov (1970) and argued that the 1/2 factor needed in [1] can be obtained theoretically from an analysis using the concept of the fastest growing wave. There is some uncertainty in their argument, however, since their analysis shows that the wavelength that has the largest growth rate also requires the largest gas velocity to induce instability. In other words, a lower gas velocity could theoretically induce instability at wavelengths that do not grow as fast.

This paper reexamines the growth of small amplitude long wavelength disturbances. The approach differs from classical Kelvin–Helmholtz linear stability theory in that liquid phase viscous and inertia terms are included. Furthermore, the notion of an inviscid plug flow in the gas is abandoned so that shear stresses at the gas–liquid interface and the component of the pressure out of phase with the wave height are considered. The inclusion of these extra effects causes the wave velocity to be greater than the average liquid velocity at neutral stability instead of being equal to it, as would be the case for classical Kelvin–Helmholtz instability. The consequence of this is that inertia terms become destabilizing, thus causing the instability to occur at a lower gas velocity than would be predicted by [1]. The results of this analysis are compared to observations of the onset of slugging for air–water flow in horizontal 2.54- and 9.53-cm transparent pipes with lengths of 15.2 and 24.6 m, respectively.

The method of analysis used in this paper is similar to approaches taken by Hanratty & Hershman (1961) and by Andreussi *et al.* (1983). These papers and a recent review article by Hanratty (1983) should be consulted for details not presented here.

2. VISCOUS INSTABILITY-CHANNEL FLOW

(a) *The stability relations*

The system considered is a cocurrent flow of a gas and a liquid layer of height h in a rectangular channel of height B, inclined at an angle, θ, to the vertical as depicted in figure 1. Average liquid and gas velocities are defined as

$$u_a=\frac{1}{h}\int_0^h u\,\mathrm{d}y, \qquad [5]$$

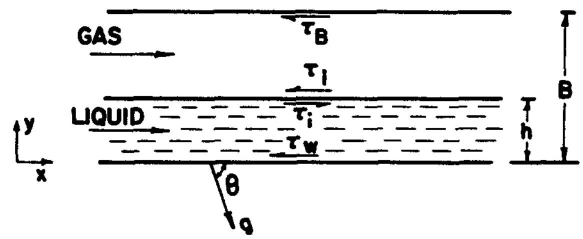

Figure 1. Diagram of system.

$$U_a = \frac{1}{B-h}\int_h^B U\,\mathrm{d}y, \tag{6}$$

where u,U are local velocities and y is the distance from the bottom wall. The shear stresses at the channel walls and at the gas–liquid interface are designated as τ_B, τ_W and τ_i. The goal of the analysis is to determine the conditions under which a small amplitude long wavelength sinusoidal disturbance introduced at the interface becomes unstable.

Because the wavelength is considered to be very large compared to h, a shallow liquid assumption can be made whereby the local pressure in the liquid, p, varies in the y-direction only because of changes in hydrostatic head. If surface tension effects are neglected, this assumption can be expressed as

$$p = P_i + \rho_L g\,(h - y)\sin\theta, \tag{7}$$

with P_i being the gas pressure at the interface. The flow field in the liquid is described by the following integral forms of the mass and momentum balances:

$$\frac{\partial h}{\partial t} + \frac{\partial}{\partial x}(hu_a) = 0, \tag{8}$$

$$\frac{\partial(hu_a)}{\partial t} + \frac{\partial}{\partial x}(h\Gamma u_a^2) = -\frac{h}{\rho_L}\left(\frac{\partial P_i}{\partial x} + \rho_L g\sin\theta\frac{\partial h}{\partial x}\right) + \frac{1}{\rho_L}(\tau_i - \tau_W) + gh\cos\theta, \tag{9}$$

where x is the coordinate in the flow direction and Γ is a shape factor defined as

$$\Gamma = \frac{1}{hu_a^2}\int_0^h u^2\,\mathrm{d}y. \tag{10}$$

Similar equations can be written for the gas phase if the wavelength of the interfacial disturbance is also considered to be very long compared to $(B - h)$. Therefore, the integral forms of the equations of conservation of mass and momentum are as follows:

$$-\frac{\partial h}{\partial t} + \frac{\partial}{\partial x}[(B-h)\,U_a] = 0, \tag{11}$$

$$\begin{aligned}\frac{\partial}{\partial t}[(B-h)\,U_a] &+ \frac{\partial}{\partial x}[(B-h)\,U_a^2\Gamma_G]\\ &= -\frac{B-h}{\rho_G}\left(\frac{\partial P_i}{\partial x} + \rho_G g\sin\theta\frac{\partial h}{\partial x}\right) - \frac{1}{\rho_G}(\tau_i + \tau_B) + g(B-h)\cos\theta,\end{aligned} \tag{12}$$

where Γ_G is the shape factor for the gas phase velocity profile.

The flow is defined by $\bar{h}$, $\bar{u}_a$ and $\bar{U}_a$ before a disturbance of the form

$$h' = \hat{h}\exp i\,k\,(x - Ct) \tag{13}$$

is introduced at the interface. The wave number k and the amplitude $\hat{h}$ characterizing the disturbance are real. The wave velocity C is complex, i.e. $C = C_R + iC_I$. The undisturbed flow is assumed to be fully developed or to be varying so slowly in the x-direction that inertia effects in [9] can be neglected:

$$0 = -\frac{\bar{h}}{\rho_L}\left(\frac{\partial \bar{P}_i}{\partial x} + \rho_L g \sin\theta \frac{\mathrm{d}\bar{h}}{\mathrm{d}x}\right) + \frac{1}{\rho_L}(\bar{\tau}_i - \bar{\tau}_W) + g\bar{h}\cos\theta. \qquad [14]$$

If the amplitude $\hat{h}$ is small enough a linear response is obtained whereby the disturbances in the velocity and stress fields are given by

$$\frac{u'_a}{\hat{u}_a} = \frac{U'_a}{\hat{U}_a} = \frac{\tau'_W}{\hat{\tau}_W} = \frac{\tau'_B}{\hat{\tau}_B} = \frac{\tau'_i}{\hat{\tau}_i} = \frac{P'_i}{\hat{P}_i} = \exp ik(x - Ct), \qquad [15]$$

with the amplitudes, $\hat{u}_a$, $\hat{U}_a$, $\hat{\tau}_W$, $\hat{\tau}_B$, $\hat{\tau}_i$, $\hat{P}_i$ being complex and linearly dependent on $\hat{h}$.

The substitution of [13] and [15] into linearized forms of [8] and [11] gives the relations for $\hat{u}_a$ and $\hat{U}_a$.

$$\frac{\hat{u}_a}{\hat{h}} = \frac{(C - \bar{u}_a)}{\bar{h}}, \qquad [16]$$

$$\frac{\hat{U}_a}{\hat{h}} = \frac{(\bar{U}_a - C)}{(B - \bar{h})}. \qquad [17]$$

The substitution of [13], [15] and [16] into a linearized form of the liquid momentum balance gives the following two equations describing neutral stability ($C_I = 0$):

$$\left(\frac{C_R}{\bar{u}_a}\right)^2 - 2\bar{\Gamma}\left(\frac{C_R}{\bar{u}_a}\right) - \bar{h}\frac{\hat{\Gamma}_R}{\hat{h}} + \bar{\Gamma} = -\frac{1}{\rho_L k \bar{u}_a^2}\left(\frac{\hat{\tau}_{iI}}{\hat{h}} - \frac{\hat{\tau}_{WI}}{\hat{h}}\right) + \frac{\bar{h}}{\rho_L \bar{u}_a^2}\left(\frac{\hat{P}_{iR}}{\hat{h}} + \rho_L g \sin\theta\right), \qquad [18]$$

$$\left(\frac{\hat{\tau}_{iR}}{\hat{h}} - \frac{\hat{\tau}_{WR}}{\hat{h}}\right) - \left(\frac{\bar{\tau}_i}{\bar{h}} - \frac{\bar{\tau}_W}{\bar{h}}\right) + k\bar{h}\frac{\hat{P}_{iI}}{\hat{h}} + (2\bar{\Gamma} - 1)\left(\frac{C_R}{\bar{u}_a} - 1\right)\rho_L \frac{\bar{u}_a^2}{\bar{h}}\frac{\mathrm{d}\bar{h}}{\mathrm{d}x} = 0. \qquad [19]$$

The terms on the left side of [18] originate from the inertia terms in [9]. As will be shown later, the stress terms $\hat{\tau}_{iL}$ and $\hat{\tau}_{WI}$ can be neglected. Consequently [18] indicates that instability occurs when the stabilizing effect of gravity is counterbalanced by the destabilizing effects of inertia and of the Bernoulli effect, represented by $\hat{P}_{iR}/\hat{h}$. The magnitude of the inertia effects depends on C_R, which is defined by [19].

(b) *Evaluation of* $\hat{\mathrm{P}}_{\mathrm{i}}$

The substitution of [13], [15] and [17] into a linearized form of the gas phase momentum balance, [12], gives expressions for $\hat{P}_{iR}$ and $\hat{P}_{iI}$.

$$\frac{\hat{P}_{iR}}{\hat{h}} = \frac{\rho_G}{(B - \bar{h})}\left[C_R^2(\bar{\Gamma}_G - 1) - \bar{\Gamma}_G(\bar{U}_a - C_R)^2 - \bar{U}_a^2(B - \bar{h})\frac{\hat{\Gamma}_{GR}}{\hat{h}} - (B - \bar{h})\, g\sin\theta - \frac{1}{k\rho_G}\left(\frac{\hat{\tau}_{iI}}{\hat{h}} + \frac{\hat{\tau}_{BI}}{\hat{h}}\right)\right], \qquad [20]$$

$$\frac{\hat{P}_{iI}}{\hat{h}} = \frac{\rho_G}{(B - \bar{h})}\left[\frac{\bar{\tau}_B + \bar{\tau}_i}{\rho_G k(B - \bar{h})} + \left(\frac{\hat{\tau}_{iR}}{\hat{h}} + \frac{\hat{\tau}_{BR}}{\hat{h}}\right)\frac{1}{\rho_G k} + \frac{(2\Gamma_G - 1)(\bar{U}_a - C_R)\,\bar{U}_a}{(B - \bar{h})\,k}\frac{\mathrm{d}\bar{h}}{\mathrm{d}x}\right]. \qquad [21]$$

(c) *Evaluation of* $\hat{\tau}_i$ *and* $\hat{\tau}_B$

Because of the assumption of a long wavelength disturbance the shear stresses are evaluated by using a pseudosteady state approximation, whereby the instantaneous stress is related to flow variables by equations derived for the undisturbed flow.

$$\tau_i = \tfrac{1}{2}\rho_G f_i (U_a - C_R)^2, \qquad [22]$$

$$\tau_B = \tfrac{1}{2}\rho_G f_B (U_a)^2. \qquad [23]$$

The friction factor f_B is given by the Blasius equation for a smooth surface,

$$f_B = f_S = 0.0665\ \mathrm{Re}_G^{-1/4}, \qquad [24]$$

with $\mathrm{Re}_G = (B - h)\,U_a/\nu_G$. The friction factor f_i is affected by the small scale wave structure on the interface and therefore depends on the flow properties of the liquid.

The following equations are derived from [22] and [24] by using procedures outlined by Hanratty (1983):

$$\frac{\hat{\tau}_{iR}}{\hat{h}} = \left[\frac{2}{B - \bar{h}} + \frac{C_R}{\bar{u}_a}\frac{\overline{\mathrm{Re}}_L}{\bar{f}_i}\left(\frac{\partial \bar{f}_i}{\partial \overline{\mathrm{Re}}_L}\right)\frac{1}{\bar{h}}\right]\bar{\tau}_i, \qquad [25]$$

$$\frac{\hat{\tau}_{BR}}{\hat{h}} \simeq \frac{2\bar{\tau}_B}{(B - \bar{h})}, \qquad [26]$$

$$\hat{\tau}_{iI} = \hat{\tau}_{BI} = 0. \qquad [27]$$

(d) *Evaluation of* $\hat{\tau}_W$ *and* $\hat{\Gamma}$

For cases in which the liquid is turbulent the shape factor for the liquid is approximated by assuming

$$\hat{\Gamma} = 0. \qquad [28]$$

The wall shear stress is defined by

$$\tau_W = \tfrac{1}{2}\rho_L f_W u_a^2, \qquad [29]$$

with

$$f_W = 0.0665\ \mathrm{Re}_L^{-1/4}. \qquad [30]$$

From [15], [29] and [30] the following relations are derived:

$$\hat{\tau}_{WI} = 0, \qquad [31]$$

$$\frac{\hat{\tau}_{WR}}{\hat{h}} = \frac{\bar{\tau}_W}{\bar{h}}\left[1.75\frac{C_R}{\bar{u}_a} - 2\right]. \qquad [32]$$

Lin (1984) has explored a more rigorous method for evaluating $\hat{\tau}_W$ and $\hat{\Gamma}$ for a sheared turbulent liquid, which involved the use of the van Driest mixing length relation. No significant difference was noted from the simple plug flow relation given above over the range of flow variables explored in this paper.

Hanratty (1983) presents the following relations for the case in which the liquid is in laminar flow:

$$\tau_W = \frac{2\mu_L u_a}{h} - \frac{h\tilde{P}}{3}, \qquad [33]$$

$$\Gamma = \frac{4}{3} + \frac{P}{18} + \frac{P^2}{270}, \qquad [34]$$

with $\tilde{P} = \mathrm{d}p/\mathrm{d}x - \rho_L g \cos\theta$ and $P = h^2\tilde{P}/\mu_L u_a$. Relations for $\hat{\tau}_W$ and $\hat{\Gamma}$ are obtained from [33] and [34] by making a pseudo-steady-state assumption:

$$\frac{\hat{\tau}_{WR}}{\hat{h}} = \frac{3\mu_L \bar{u}_a}{\bar{h}^2}\left(\frac{C_R}{\bar{u}_a} - 2\right) - \frac{1}{2}\frac{\hat{\tau}_{iR}}{\hat{h}}, \qquad [35]$$

$$\frac{\hat{\tau}_{WI}}{\hat{h}} = -\frac{1}{2}\frac{\hat{\tau}_{iI}}{\hat{h}}, \qquad \frac{\hat{\Gamma}_I}{\hat{h}} = 0, \qquad [36]$$

$$270\,\bar{h}\frac{\hat{\Gamma}_R}{\hat{h}} = \left(2 - \frac{C_R}{\bar{u}_a}\right)(2P + 15)(P + 3) + \frac{3}{2}P\frac{\hat{\tau}_{iR}}{\bar{\tilde{P}}\hat{h}}(2P + 15). \qquad [37]$$

3. CONDITIONS FOR NEUTRAL STABILITY FOR TURBULENT–TURBULENT FLOW IN A CHANNEL

The substitution of [20], [21], [25], [26], [27], [28], [31], [32] into [18] yields the following equation for neutral stability

$$\frac{\bar{V}_{SL}^2}{g\,B\sin\theta}\frac{1}{(1 - \alpha)^3}\left(\frac{C_R}{\bar{u}_a} - 1\right)^2 + \frac{\bar{V}_{SG}^2}{g\,B\sin\theta}\frac{\rho_G}{\rho_L}\frac{1}{\alpha^3} - \left(\frac{\rho_L - \rho_G}{\rho_L}\right) = 0. \qquad [38]$$

Here $\bar{V}_{SG}$ and $\bar{V}_{SL}$ are the superficial velocities and α is the void fraction, $\alpha = (B - \bar{h})/B$, and $\bar{\Gamma} = \bar{\Gamma}_G = 1$ for turbulent flows.

The first term in [38] represents the destabilizing effect of liquid inertia. The second is the destabilizing effect of gas phase pressure variations. The third is the stabilizing effect of gravity. For the case of $C_R/\bar{u}_a = 1$, liquid inertia effects vanish and [1] is obtained. It is seen that liquid inertia causes the transition velocity to be smaller. In order to estimate this effect [19] has to be used to evaluate $C_R/\bar{u}_a$.

The substitution of [20], [21], [25], [26], [27], [28], [31], [32] into [19] gives

$$\frac{C_R}{\bar{u}_a} = \frac{3 + \left(\frac{1-\alpha}{\alpha}\right)^2\left(3\,\bar{\tau}_i^+(1 + \phi) + \frac{2}{\bar{f}_i}\frac{\mathrm{d}\bar{h}}{\mathrm{d}x}\right) + \bar{\tau}_i^+\left[2\left(\frac{1-\alpha}{\alpha}\right) - 1\right] - \frac{2}{\bar{f}_W}\frac{\mathrm{d}\bar{h}}{\mathrm{d}x}}{2 - 0.25 - \bar{\tau}_i^+\,\Psi\left(1 + \frac{1-\alpha}{\alpha}\right) + \frac{2}{\bar{f}_W}\frac{\mathrm{d}\bar{h}}{\mathrm{d}x}}, \qquad [39]$$

where

$$\phi = \frac{\bar{\tau}_B}{\bar{\tau}_i} \simeq (f_i/f_s)^{-1}, \qquad [40]$$

$$\bar{\tau}_i^+ = \bar{\tau}_i/\bar{\tau}_W, \qquad [41]$$

$$\Psi = \frac{\overline{\mathrm{Re}}_L}{\bar{f}_i}\frac{\partial \bar{f}_i}{\partial \overline{\mathrm{Re}}_L}. \qquad [42]$$

It is noted that terms involving $\mathrm{d}\bar{h}/\mathrm{d}x$ are small so the following equation is applicable both for a fully developed flow and for a flow with a slight hydraulic gradient:

$$\frac{C_R}{\bar{u}_a} = \frac{3 + 3\left(\frac{1-\alpha}{\alpha}\right)^2(\bar{\tau}_i^+)(1 + \phi) + \bar{\tau}_i^+\left[2\left(\frac{1-\alpha}{\alpha}\right) - 1\right]}{1.75 - \bar{\tau}_i^+\,\Psi\left(1 + \frac{1-\alpha}{\alpha}\right)}. \qquad [43]$$

From [22], [24], [29], [30],

$$\bar{\tau}_i^+ = \left(\frac{\rho_G}{\rho_L}\right)\left(\frac{V_{SG}}{V_{SL}}\right)^{1.75}\left(\frac{1-\alpha}{\alpha}\right)^2\left(\frac{f_i}{f_s}\right)\left(\frac{\nu_G}{\nu_L}\right)^{1/4}. \qquad [44]$$

As suggested by Andreussi *et al.* (1983), the ratio of the friction factor for a wave roughened interface to that for a smooth surface can be approximated by

$$f_i/f_s \simeq 1 + \beta h_G^+, \qquad [45]$$

where $h_G^+ = hU_G^*/\nu_G$, with $U_G^* = (\tau_i/\rho_G)^{1/2}$. From [45],

$$\Psi \simeq \frac{\bar{f}_i/\bar{f}_s - 1}{\bar{f}_i/\bar{f}_s}. \qquad [46]$$

From [43], [44], [46] it is seen that $C_R/\bar{u}_a$ is a function of $\alpha, f_i/f_s, \nu_{SG}, \nu_{SL}, \rho_G/\rho_L, \nu_G/\nu_L$. The term f_i/f_s can be approximated by [45] and all the terms except α are defined by the operating conditions for the channel. In general, measured values of α should be used. However, for the case in which the flow is fully developed a relation between α and the other flow variables can be derived. For this case $(\mathrm{d}\bar{h}/\mathrm{d}x = 0)$ it follows from [14] that

$$\bar{\tau}_i^+ = \frac{1 + \left(\dfrac{\rho_L - \rho_G}{\rho_L}\right)\dfrac{2}{\bar{f}_W}\dfrac{gB}{V_{SL}^2}(1-\alpha)^3\cos\theta}{\left[1 + (1+\phi)\left(\dfrac{1-\alpha}{\alpha}\right)\right]}, \qquad [47]$$

with f_w given by [30]. The elimination of $\bar{\tau}_i^+$ between [44] and [47] gives a relation between α and V_{SL}, V_{SG}.

For a fully developed horizontal flow $(\theta = \pi/2)$, [44] and [47] give the following relation between V_{SG}/V_{SL} and α:

$$\left(\frac{V_{SG}}{V_{SL}}\right)^{1.75} = \left[1 + (1+\phi)\left(\frac{1-\alpha}{\alpha}\right)\right]^{-1}\left[\frac{\rho_G}{\rho_L}\left(\frac{f_i}{f_s}\right)\left(\frac{\nu_G}{\nu_L}\right)^{1/4}\left(\frac{1-\alpha}{\alpha}\right)^2\right]^{-1}. \qquad [48]$$

Equation [38] then gives the following condition for neutral stability if [48] is used to eliminate V_{SG}/V_{SL}:

$$\frac{V_{SG}}{\sqrt{gB}}\sqrt{\frac{\rho_G}{\rho_L - \rho_G}} = K\alpha^{3/2}, \qquad [49]$$

with

$$\frac{1}{K^2} = 1 + \left(\frac{\alpha}{1-\alpha}\right)^{0.714}\left(\frac{C_R}{\bar{u}_a} - 1\right)^2\left[1 + (1+\phi)\left(\frac{1-\alpha}{\alpha}\right)\right]^{1.14}\left(\frac{\rho_G}{\rho_L}\right)^{0.143}\left(\frac{f_i}{f_s}\right)^{1.17}\left(\frac{\nu_G}{\nu_L}\right)^{0.286}. \qquad [50]$$

From [47], [48] and [43] it is found that $C_R/\bar{u}_a$, and therefore K, is a function of $\alpha, f_i/f_s$ and fluid properties for a fully developed flow.

Figure 2 is a plot of calculated neutral stability conditions for a fully developed air–water flow $(\rho_G/\rho_L = 1.12 \times 10^{-3}, \nu_G/\nu_L = 16.1)$. It is noted that the predicted critical V_{SG} are much smaller than those given by inviscid Kelvin–Helmholtz analysis, [1].

Figure 3 presents the calculated transition for the fully developed turbulent–turbulent case in the more familiar Mandhane coordinates of V_{SL} vs V_{SG} for the case of a channel with

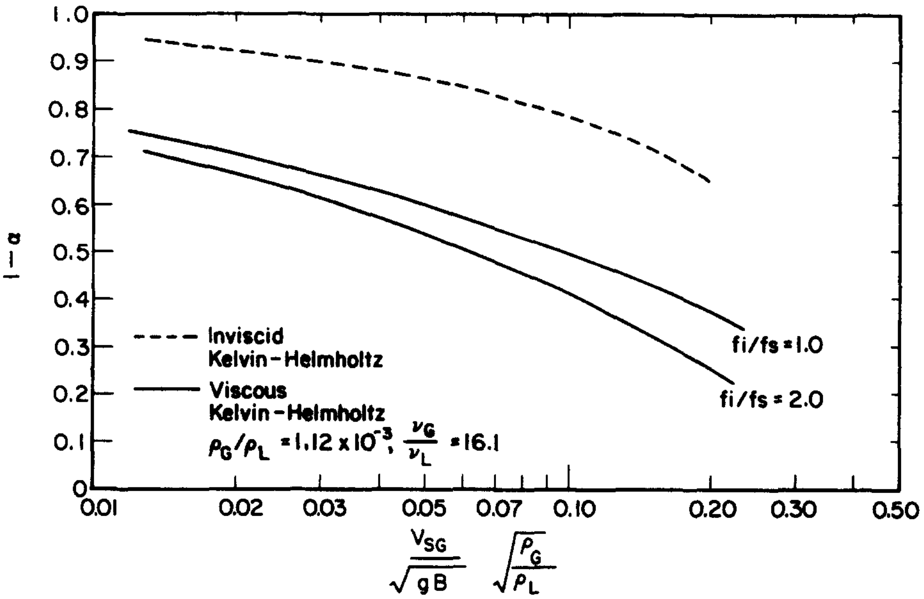

Figure 2. Neutral stability conditions for fully developed horizontal air–water flow in a channel.

$B = 2.54$ cm. Equation [48] was used to calculate V_{SL} from α and V_{SG} for the inviscid Kelvin–Helmholtz prediction. Again it is seen that for fixed V_{SG}, the predicted transition occurs for lower values of V_{SL} than predicted by the inviscid Kelvin–Helmholtz theory.

4. EFFECT OF LIQUID VISCOSITY ON NEUTRAL STABILITY IN A CHANNEL

(a) *Stability equations for a turbulent gas–laminar liquid flow*

The influence of liquid viscosity on stability for a turbulent–turbulent flow is weak. However, flows with very large liquid viscosities would involve a laminar liquid flow. More interesting effects of liquid viscosity are obtained by examining the stability of a turbulent gas–laminar liquid.

The substitution of [20], [21], [25], [26], [27], [35], [36], in [18] gives the following neutral stability condition:

$$\frac{V_{SL}^2}{g\,B\sin\theta}\frac{\Omega}{(1-\alpha)^3}+\frac{V_{SG}^2}{g\,B\sin\theta}\frac{\rho_G}{\rho_L}\frac{1}{\alpha^3}-\left(\frac{\rho_L-\rho_G}{\rho_L}\right)=0, \qquad [51]$$

$$\Omega=\left(\frac{C_R}{\bar{u}_a}\right)^2-2\,\bar{\Gamma}\left(\frac{C_R}{\bar{u}_a}\right)+\bar{\Gamma}-\bar{h}\,\hat{\Gamma}_R. \qquad [52]$$

It is noted that this is very similar to the neutral stability condition for a turbulent–turbulent flow, with $\bar{\Gamma}$ and $\hat{\Gamma}_R/\hat{h}$ defined by [34] and [37].

An examination of [51] reveals two effects of an increase in viscosity. For a fixed $\bar{V}_{SG}$ and α, $\bar{V}_{SL}$ for the undisturbed flow will decrease with an increase in liquid viscosity (see [57]). From this consideration, the second term in [51] would suggest a transition at a smaller value of $\bar{V}_{SL}$. However, a smaller $\bar{V}_{SL}$ reduces the destabilizing effects of inertia given by the first term in [51] and this tends to counterbalance the above effect. For very large viscosities inertia effects will be negligible and [1] will define neutral stability.

The following equation for $C_R/\bar{u}_a$ is obtained from [19], [22], [23] for a laminar liquid by using [33]–[37] and the assumption of a smooth surface ($f_i/f_s = 1$):

$$\frac{C_R}{\bar{u}_a}=\frac{6-P}{9}\left\{\left(\frac{18}{6-P}+1\right)+6\left(\frac{1-\alpha}{\alpha}\right)^2\bar{\tau}_i^{+}+\bar{\tau}_i^{+}\left[3\left(\frac{1-\alpha}{\alpha}\right)-1\right]\right\}, \qquad [53]$$

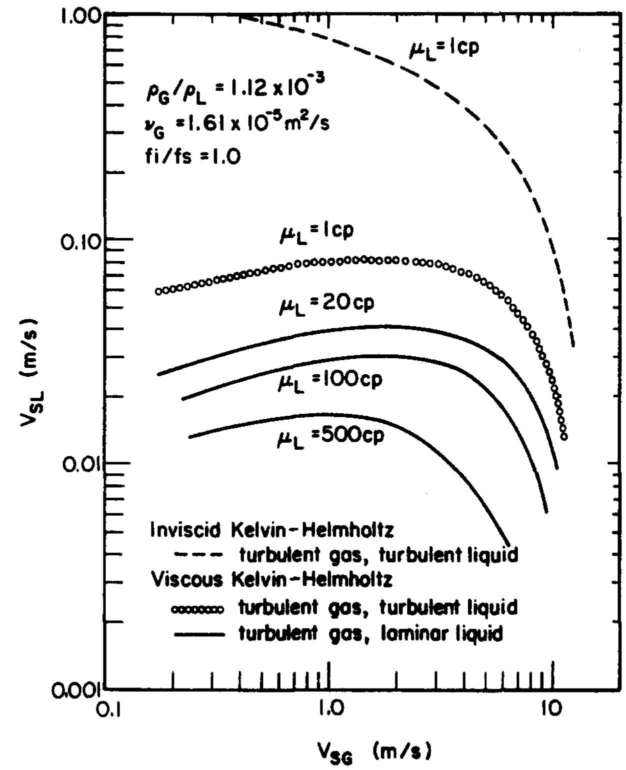

Figure 3. Effect of liquid viscosity on calculated neutral stability for fully developed horizontal channel flow with $B = 2.54$ cm.

$$P = \frac{2}{\frac{1}{3} + (\bar{\tau}_i^+ - 1)^{-1}}. \qquad [54]$$

An expression can be derived for $\bar{\tau}_i^+$ from [14] and a similar momentum balance for the gas phase. By making use of [22] and [33], it is found that

$$\frac{1}{\bar{\tau}_i^+} = \left(1 + (1 + \phi)\frac{1 - \alpha}{\alpha}\right) + \frac{2}{0.0665}\left(\frac{\rho_L}{\rho_G}\right)\left(\frac{1 - \alpha}{\alpha}\right)\left(\frac{V_{SG}^2}{gB}\right)^{-1}\left(\frac{V_{SG}B}{\nu_G}\right)^{-1/4}\cos\theta. \qquad [55]$$

The substitution of [53], [54], [55] into [51]–[52] gives the neutral stability in terms of $\bar{V}_{SL}$, $\bar{V}_{SG}$, α and fluid properties.

Using [14], [22] and [33], the following relation between α, V_{SG} and V_{SL} can be obtained:

$$-\frac{4}{3}\frac{1 - \alpha}{\alpha}\left[1 + \frac{\rho_L}{\rho_G}\left(\frac{V_{SG}B}{\nu_G}\right)^{1/4}\left(\frac{V_{SG}^2}{gB}\right)^{-1}\frac{\alpha^3\cos\theta}{0.0665}\right] = 1 - \frac{4}{0.0665}\frac{\rho_L}{\rho_G}\left(\frac{V_{SL}}{V_{SG}}\right)^2\left(\frac{\alpha}{1 - \alpha}\right)^2\left(\frac{V_{SG}B}{\nu_G}\right)^{1/4}\left(\frac{V_{SL}B}{\nu_L}\right)^{-1}. \qquad [56]$$

For the case of a horizontal flow, [56] simplifies to

$$V_{SL} = \Xi\, V_{SG}^{1.75}\, B^{3/4}\frac{\nu_G^{1/4}}{\nu_L}, \qquad [57]$$

$$\Xi = \frac{1}{60.15}\left(\frac{1 - \alpha}{\alpha}\right)^2\left[1 + \frac{4}{3}\left(\frac{1 - \alpha}{\alpha}\right)\right]\left(\frac{\rho_G}{\rho_L}\right) \qquad [58]$$

By substituting [57] into [51] the following equation is obtained for neutral stability of a fully developed horizontal laminar liquid:

$$\frac{V_{SG}}{\sqrt{gB}}\sqrt{\frac{\rho_G}{\rho_L-\rho_G}} = K_\ell\,\alpha^{3/2} \tag{59}$$

$$K_\ell = \left[1 - \frac{\Omega\,\Xi^2}{(1-\alpha)^3}\left(\frac{\nu_G^4}{\nu_L^2\,g\,B^3}\right)\left(\frac{BV_{SG}}{\nu_G}\right)^{3.5}\right]^{1/2}. \tag{60}$$

For large ν_L, $K_\ell \simeq 1$ and the neutral stability condition reduced to [1].

The influence of viscosity on the calculated neutral stability curve is illustrated in figure 3 for a fully developed horizontal turbulent gas–laminar liquid. The calculations were made for air and liquids of different viscosity flowing in a channel with $B = 2.54$ cm. It is noted that over the range of 1 to 100 cp liquid viscosity is having a mild effect on the neutral stability. This is because of its counterbalancing influence on α and on the liquid inertia. However, as the viscosity exceeds 500 cp the effects of the liquid inertia term in [51] become vanishingly small. Stability is defined by [1] and the critical V_{SL} is more strongly affected by increases of liquid viscosity.

5. COMPARISON OF THE LINEAR STABILITY ANALYSIS WITH OBSERVED TRANSITIONS TO SLUG FLOW

The principle goal of this paper was to see whether a linear stability analysis of the type presented here can explain the observed transition to slug flow. The equations developed have been used successfully to explain the transition to roll waves (Hanratty, 1983) on thin liquid layers (large α). Consequently, it is concluded that in such cases the unstable infinitesimal wave grows to a large amplitude wave having a steep front and a gradually sloping back. The main difference in the work presented here is that the analysis is extended to small values of α. The motivation is the possibility that for small α the unstable infinitesimal wave will grow sufficiently to block the pipe cross-section and form a slug. The stability theory might, therefore, describe the asymptotic behavior of the slug flow transition for small α.

There is some encouragement for this type of reasoning from recent experiments carried out by Lin (1984). These were conducted in a 2.54-cm diameter pipeline with $L/D = 600$ and in a 9.53-cm pipeline with $L/D = 260$. At gas velocities greater than about 3.3 m/s and at sufficiently high liquid velocities the formation of a slug was observed to occur by the coalescence of roll waves. However, for gas velocities less than this coalescence did not appear to explain slug formation. Consequently it was decided to compare Lin's observations at $V_{SG} < 3.3$ m/s with the stability calculations presented in this paper.

The stability analysis presented in the previous sections for a rectangular channel is developed for a circular pipe in the appendix. Calculated results from this analysis are compared with Lin's experiments in figures 4 and 5.

At low gas velocities, hydraulic gradients in the liquid exist even at $L/D = 600$ and with the pipe carefully levelled. It is therefore more accurate to compare experiments with calculations using measured values of liquid film thickness. This is done in figure 4 where actual measured values of h/D at transition are plotted against $V_{SG}\rho_G^{1/2}/(gD\rho_L)^{1/2}$ for air and water.

It is noted that the experiments agree with the stability theory in that no effect of pipe diameter is seen in such a plot. Agreement between the experiments and the stability calculations is obtained if f_i/f_s is assumed equal to 2.0. This is a reasonable assumption for air–water flow in this range of h/D (Andritsos 1985).

A comparison of the calculations for $f_i/f_s = 1.0$ with the conjecture of Taitel & Dukler (1976), represented by [3] and [4], is also presented. The good agreement would suggest that

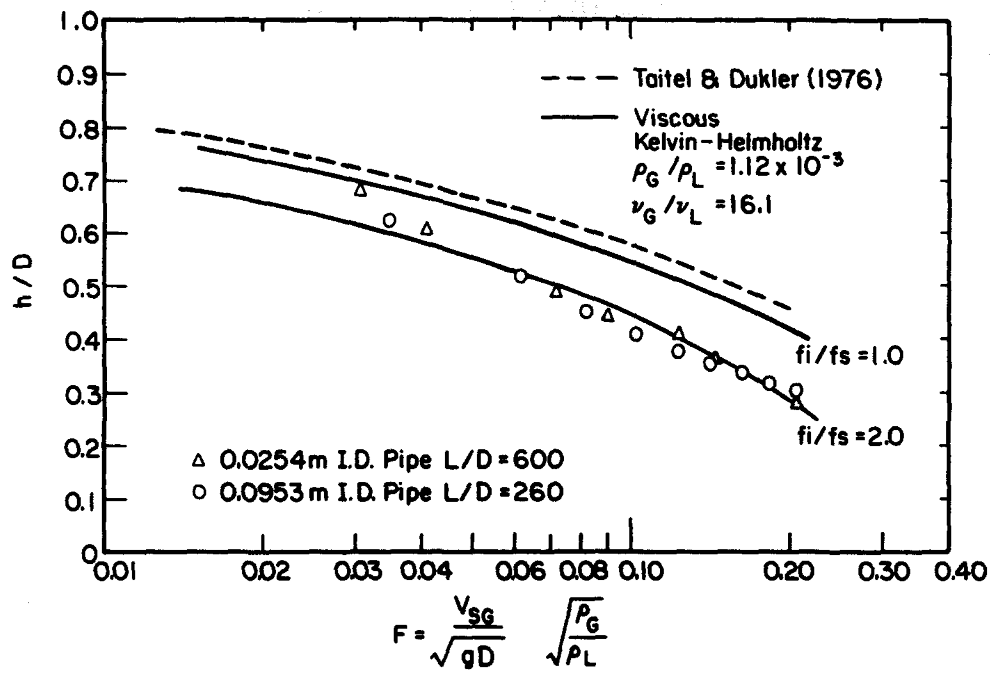

Figure 4. Comparison of stability analysis for fully developed horizontal pipe flow with Lin's (1984) experiments.

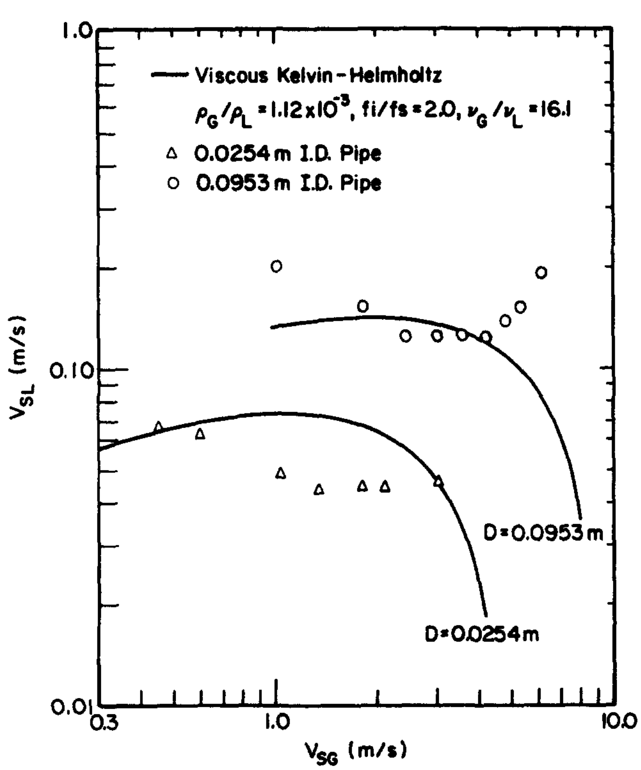

Figure 5. Comparison of stability analysis for fully developed horizontal pipe flow with Lin's (1984) experiments in Mandhane coordinates.

[4] can be interpreted as a correction for the destabilizing effect of liquid inertia for air–water flow.

Figure 5 compares Lin's measurements with stability theory (with $f_i/f_s = 2.0$) in a Mandhane plot. This plot clearly illustrates the success of figure 4 in accounting for the effect of pipe diameter. It is noted that for $V_{SG} > 7$ m/s for the 9.53-cm pipe (3 m/s for the 2.54-cm pipe) the stability calculation corresponds to an observed transition to roll waves, and not to slug flow. Larger values of V_{SL} than predicted by the stability analysis are needed to initiate slugs in this range of gas velocities.

6. CONCLUSIONS

Inviscid Kelvin–Helmholtz theory incorrectly predicts the stability of stratified gas–liquid flows in an enclosed duct to infinitesimal long wavelength disturbances. This is because viscous effects can cause the wave velocity to be quite different from the value predicted by inviscid theory. Because of this, the inertia of the liquid can be destabilizing. This provides a possible explanation of why inviscid Kelvin–Helmholtz theory predicts high critical gas velocities for the initiation of slugs in air–water flows.

The comparison of viscous linear stability theory with observations of the initiation of slugs for air–water flow in 2.54- and in 9.73-cm horizontal pipes is good provided $V_{SG} < 3.3$ m/s. This supports the notion that for thick enough liquid layers slugs result from the growth of small disturbances.

For liquid viscosities in the range of 1 to 500 cp viscous stability theory predicts a much more moderate effect of viscosity on the critical V_{SL} than what is predicted by inviscid Kelvin–Helmholtz theory, as has been suggested by Mandhane *et al.* (1974) and by Weisman *et al.* (1979). However, at very large liquid viscosities inertia effects of the liquid film are negligible and the same stability criterion is obtained from the viscous and inviscid theories.

The most widely used correlation to predict the initiation of slugs is the correction to Kelvin–Helmholtz inviscid theory introduced by Taitel & Dukler, [4]. This correction is found to account correctly for the effects of inertia for an air–water flow. However, this equation does not agree with viscous stability for liquids other than water since the correction for inertia is a complicated function of fluid viscosity as well as of h/D.

Acknowledgement—This work has been supported by the A.I.Ch.E. Design Institute for Multiphase Processing and by the Shell Companies Foundation.

NOMENCLATURE

A	cross-sectional area
B	channel height
C	wave velocity
D	pipe diameter
f	function of (h/D) in [3]
f_B, f_i, f_w	friction factors
f_s	interfacial friction factor assuming a hydraulically smooth interface
F	dimensionless superficial gas velocity defined in [3]
g	acceleration due to gravity
h, h_L	height of liquid film
h_G^+	dimensionless height of conduit occupied by gas, hU_G^*/ν_G
k	wave number

K, K_1, K_2, K_t	correction factors to inviscid Kelvin–Helmholtz solution defined in [50], [2], [3] and [59], respectively
L	pipe length
p, P	local pressure in liquid and gas phase, respectively
$\tilde{P}$	$\mathrm{d}p/\mathrm{d}x - \rho_L g \sin\theta$
P	$h^2\tilde{P}/\mu_L u_a$
$\mathrm{Re}_L, \mathrm{Re}_G$	Reynolds numbers: $u_a h/\nu_L$ and $U_a(B-h)/\nu_G$, respectively for channel flow; $u_A D_L/\nu_L$ and $U_A D_G/\nu_G$, respectively, for pipe flow.
S	round pipe geometrical parameters, defined in figure 1(A)
t	time
u	local velocity in liquid
U	local velocity in gas
V_c	gas velocity over the crest, [2]
V_{SG}, V_{SL}	superficial velocities of the gas and liquid, respectively; defined as flow rate of the individual phase divided by total cross-sectional area of the conduit
x	coordinate in direction of flow
y	coordinate perpendicular to direction of flow, measured from bottom wall
α	void fraction
β	coefficient used in [45], approximately equals to 1
γ	angle defined in figure 1A
Γ	velocity profile shape factor, [10]
θ	pipe inclination to the vertical
Ξ, Ξ_p	coefficients defined in [58] and [A55], respectively
μ	viscosity
ν	kinematic viscosity
ρ	density
τ_B, τ_i, τ_w	shear stresses
$\bar{\tau}_i^+$	$\bar{\tau}_i/\bar{\tau}_w$
ϕ	$\bar{\tau}_B/\bar{\tau}_i$, [40]
ψ	$(\overline{\mathrm{Re}}_L/\bar{f}_i)\,(\partial f_i/\partial \mathrm{Re}_L)$, [42]
ψ_L	$(\mathrm{d}f_w/\mathrm{dRe}_L)\,(\overline{\mathrm{Re}}_L/\bar{f}_w)$
Ω, Ω_p	functions of $(C_R/\bar{u}_a)$, defined in [52] and [A51], respectively

Subscripts

a	quantities spatially averaged over length as in [5] and [6]
A	quantities spatially averaged over area, as in [A15] and [A16]
B	quantities at gas side conduit wall
G	gas phase
i	at gas–liquid interface
I	imaginary part
L	liquid phase
R	real part
S	at gas–liquid interface, assuming interface is hydraulically smooth
w	at liquid side conduit wall

Superscripts

$'$	fluctuating component of perturbation
$-$	time averaged quantities
$\hat{}$	amplitude of fluctuating component of perturbation
$\tilde{}$	dimensionless round pipe geometrical quantities; made dimensionless with respect to D for lengths, and D^2 for areas

REFERENCES

AGRAWAL, S. S., GREGORY, G. A. & GOVIER, G. W. 1973 An analysis of horizontal stratified two-phase flow in pipes. *Can. J. Chem. Eng.* **51**, 280–286.

ANDREUSSI, P., ASALI, J. C. & HANRATTY, T. J. 1985 Initiation of roll waves in gas–liquid flows. *AIChE J.* **31**, 119–126.

ANDRITSOS, N., Ph.D. Dissertation, University of Illinois, Urbana, to be published.

BENJAMIN, T. B. 1968 Gravity currents and related phenomena. *J. Fluid Mech.* **31**, 209–248.

HANRATTY, T. J. 1983 Interfacial instabilities caused by air flow over a thin liquid layer. *Waves on Fluid Interfaces*, pp. 221–259. Academic, New York.

HANRATTY, T. J. & HERSHMAN, J. M. 1961 Initiation of roll waves. *AIChE J.* **7**, 488–497.

KORDYBAN, E. S. 1977 Some characteristics of high waves in closed channels approaching Kelvin-Helmholtz instability. *ASME J. Fluids Eng.* **99**, 339–346.

KORDYBAN, E. S. & RANOV, T. 1970 Mechanism of slug formation in horizontal two-phase flow. *J. Basic Eng.* **92**, 857–864.

LIN, P. Y. 1985 Flow Regime Transitions in Horizontal Gas–Liquid Flow. Ph.D. Dissertation, University of Illinois, Urbana.

MANDHANE, J. M., GREGORY, G. A. & AZIZ, K. 1974 A flow pattern map for gas–liquid flow in horizontal pipes. *Int. J. Multiphase Flow* **1**, 537–553.

MISHIMA, K. & ISHII, M. 1980 Theoretical prediction of onset of horizontal slug flow. *J. Fluids Eng., ASME Trans.* **102**, 441–445.

TAITEL Y. & DUKLER, A. E. 1976. A model for predicting flow regime transitions in horizontal and near horizontal gas–liquid flow. *AIChE J.* **22**, 47–55.

WALLIS, G. B. & DOBSON, J. E. 1973 The onset of slugging in horizontal stratified air–water flow. *Int. J. Multiphase Flow* **1**, 173–193.

WEISMAN, J., DUNCAN, D., GIBSON, J. & CRAWFORD, T. 1979. Effects of fluid properties and pipe diameter on two-phase flow patterns in horizontal lines. *Int. J. Multiphase Flow* **5**, 437–462.

APPENDIX: VISCOUS INSTABILITY FOR A PIPE FLOW

(a) *Linearized mass and momentum balances*

The instability analysis can be extended to flow in a pipe by incorporating the appropriate geometric parameters. The special case of turbulent plug flow in both phases is used to simplify the analysis. The geometric parameters are defined according to figure 1(A). Terms A_L and A_G are the cross-sectional areas occupied by the liquid and gas phases, respectively. The geometric quantities shown in figure 1(A) are related as follows:

$$\tilde{h} = h/D, \qquad \text{[A1]}$$

$$\gamma = 2\cos^{-1}(1 - 2\tilde{h}), \qquad \text{[A2]}$$

$$\tilde{S}_i = \sqrt{\tilde{h} - (\tilde{h})^2} \qquad \text{[A3]}$$

$$\tilde{S}_L = \cos^{-1}(1 - 2\tilde{h}), \qquad \text{[A4]}$$

$$\tilde{S}_G = \pi - \tilde{S}_L, \qquad \text{[A5]}$$

$$\tilde{A}_L = \frac{1}{4}[\tilde{S}_L - \tilde{S}_i(1 - 2\tilde{h})], \qquad \text{[A6]}$$

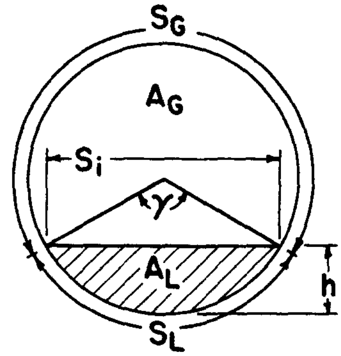

Figure 1(A). Geometric parameters for pipe flow.

$$\tilde{A}_G = \frac{\pi}{4} - \tilde{A}_L. \qquad [A7]$$

The quantities with superscript (~) are made dimensionless with respect to D, the pipe diameter, for lengths, and with respect to D^2 for areas. It is noted that all the parameters can be expressed as a function of $\tilde{h}$ alone.

If each geometric quantity is expressed as the sum of an averaged component and a fluctuating component, then the amplitudes of the fluctuations of these parameters can be expressed as

$$\frac{\tilde{S}_i}{\tilde{h}} = \frac{\hat{\tilde{S}}_i}{\hat{\tilde{h}}} = \frac{2(1-2\bar{\tilde{h}})}{\bar{\tilde{S}}_i} \qquad [A8]$$

$$\frac{\hat{\tilde{S}}_L}{\hat{\tilde{h}}} = \frac{2}{\bar{\tilde{S}}_i} \qquad [A9]$$

$$\frac{\hat{\tilde{S}}_G}{\hat{\tilde{h}}} = -\frac{\hat{\tilde{S}}_L}{\hat{\tilde{h}}} \qquad [A10]$$

$$\left(\frac{\hat{\tilde{A}}_L}{\hat{\tilde{h}}}\right) = \frac{1}{4}\left[\left(\frac{\hat{\tilde{S}}_L}{\hat{\tilde{h}}}\right) + 2\bar{\tilde{S}}_i - (1-2\bar{\tilde{h}})\left(\frac{\hat{\tilde{S}}_i}{\hat{\tilde{h}}}\right)\right]. \qquad [A11]$$

The neutral stability equations are developed in the same manner as for a channel flow. The shallow liquid assumption is also used,

$$p = P_i + \rho_L(h-y)g\sin\theta. \qquad [A12]$$

The liquid mass and momentum balances in a pipe can be written as

$$\frac{\partial A_L}{\partial t} + \frac{\partial(u_A A_L)}{\partial x} = 0 \qquad [A13]$$

$$\frac{\partial(u_A A_L)}{\partial t} + \frac{\partial(u_A^2 A_L)}{\partial x} = -\frac{A_L}{\rho_L}\left(\frac{\partial P_i}{\partial x} + \rho_L g\sin\theta\frac{\partial h}{\partial x}\right) + \frac{1}{\rho_L}(\tau_i S_i - \tau_W S_L) + A_L g\cos\theta. \qquad [A14]$$

The subscript A for the liquid velocity indicates the quantity is averaged over the cross-section of the pipe.

The amplitudes of the wave induced variations of u_A and U_A are related to the amplitudes of the area variations by using the mass balances of the two phases:

$$\hat{u}_A = \frac{C - \bar{u}_A}{\bar{A}_L} \hat{A}_L, \qquad \text{[A15]}$$

$$\hat{U}_A = \frac{\bar{U}_A - C}{A - \bar{A}_L} \hat{A}_L. \qquad \text{[A16]}$$

The governing equations for neutral stability in nonfully developed pipe flow with inclination θ are as follows:

$$\left[\left(\frac{C_R}{\bar{u}_a}\right)^2 - 2\left(\frac{C_R}{\bar{u}_A}\right) + 1\right] \hat{A}_L = \frac{-1}{\rho_L k \bar{u}_A^2} [\bar{S}_i \hat{\tau}_{iI} - \bar{S}_L \hat{\tau}_{WI}] + \frac{\bar{A}_L}{\rho_L \bar{u}_A^2} [\hat{P}_{iR} + \rho_L g \sin\theta \hat{h}] \qquad \text{[A17]}$$

and

$$(\bar{S}_i \hat{\tau}_{iR} - \bar{S}_L \hat{\tau}_{WR}) + \left[(\bar{\tau}_i \hat{S}_i - \bar{\tau}_W \hat{S}_L) + \frac{\hat{A}_L}{\bar{A}_L} (\bar{\tau}_W \bar{S}_L - \bar{\tau}_i \bar{S}_i)\right] + k \bar{A}_L \hat{P}_{iI} + \left(\frac{C_R}{\bar{u}_A} - 1\right) \frac{\mathrm{d}\hat{A}_L}{\mathrm{d}x} = 0. \qquad \text{[A18]}$$

The pressure variation in the gas is again obtained from the gas phase momentum and mass balances by using a shallow gas assumption:

$$\hat{P}_{iR} = \frac{\rho_G}{A - \bar{A}_L} \left[-\hat{A}_L (\bar{U}_A - C_R)^2 - \frac{1}{k \rho_G} (\bar{S}_i \hat{\tau}_{iI} + \bar{S}_G \hat{\tau}_{BI})\right] \qquad \text{[A19]}$$

$$\hat{P}_{iI} = \frac{\rho_G}{A - \bar{A}_L} \left(\hat{A}_L \frac{\bar{U}_A (\bar{U}_A - C_R)}{(A - \bar{A}_L)} \frac{\mathrm{d}\bar{A}_L}{\mathrm{d}x} + \frac{\bar{S}_i \bar{\tau}_i + \bar{\tau}_B \bar{S}_G}{\rho_G k (A - \bar{A}_L)} \hat{A}_L + \frac{1}{k \rho_G} (\bar{S}_i \hat{\tau}_{iR} + \bar{S}_G \hat{\tau}_{BR} + \bar{\tau}_i \hat{S}_i + \bar{\tau}_B \hat{S}_G)\right). \qquad \text{[A20]}$$

(b) *Evaluation of $\hat{\tau}_W$ for pipe flows*

The liquid phase is modeled as a turbulent plug flow with the friction factor given by the Blasius equation. As suggested by Agrawal *et al.* (1973), the liquid is treated as in open channel flow. The hydraulic diameter, D_L, is given by

$$D_L = \frac{4A_L}{S_L} \qquad \text{[A21]}$$

and the Reynolds number, Re_L, is defined as

$$\mathrm{Re}_L = \frac{D_L u_A}{\nu_L}. \qquad \text{[A22]}$$

The wall shear stress and its fluctuation are given by

$$\tau_W = \frac{1}{2} \rho_L f_W u_A^2 \qquad \text{[A23]}$$

and

$$\frac{\hat{\tau}_W}{\bar{\tau}_W} = 2\left(\frac{\hat{u}_A}{\bar{u}_a}\right) + \frac{\hat{f}_W}{\bar{f}_W}. \qquad \text{[A24]}$$

The wall friction factor is given by

$$f_W = 0.0791\ \mathrm{Re}_L^{-1/4}. \qquad \text{[A25]}$$

Hence

$$\frac{\hat{f}_W}{\bar{f}_W} = \left(\frac{\mathrm{d}\bar{f}_W}{\mathrm{d}\overline{\mathrm{Re}}_L}\right)\left(\frac{\hat{\mathrm{Re}}_L}{\bar{f}_W}\right). \qquad \text{[A26]}$$

From [A21] and [A1] through [A11],

$$\frac{\hat{D}_L}{\bar{D}_L} = \frac{\hat{A}_L}{\bar{A}_L} - \frac{(\hat{S}_L + \hat{S}_i)}{\bar{S}_L + \bar{S}_i}. \qquad \text{[A27]}$$

Equations [A15], [A22] and [A27] lead to

$$\frac{\hat{\mathrm{Re}}_L}{\overline{\mathrm{Re}}_L} = \left(\frac{C}{\bar{u}_A}\frac{\hat{A}_L}{\bar{A}_L} - \frac{\hat{S}_L}{\bar{S}_L}\right). \qquad \text{[A28]}$$

The amplitude of the wave-induced variation of τ_W is obtained from [A24], [A15], [A26], [A28]:

$$\begin{aligned}\frac{\hat{\tau}_{WR}}{\bar{\tau}_W} &= \left(\frac{C_R}{\bar{u}_A}\right)\left(2 + \frac{\mathrm{d}\bar{f}_W}{\mathrm{d}\overline{\mathrm{Re}}_l}\frac{\overline{\mathrm{Re}}_L}{\bar{f}_W}\right)\frac{\hat{A}_L}{\bar{A}_L} - 2\frac{\hat{A}_L}{\bar{A}_L} - \frac{\mathrm{d}\bar{f}_W}{\mathrm{d}\overline{\mathrm{Re}}_L}\frac{\overline{\mathrm{Re}}_L}{\bar{f}_W}\frac{\hat{S}_L}{\bar{S}_L} \\ &= 1.75\left(\frac{C_R}{\bar{u}_A}\right)\frac{\hat{A}_L}{\bar{A}_L} - 2\frac{\hat{A}_L}{\bar{A}_L} + \frac{1}{4}\frac{\hat{S}_L}{\bar{S}_L}\end{aligned} \qquad \text{[A29]}$$

$$\frac{\hat{\tau}_{WI}}{\bar{\tau}_W} = 0 \qquad \text{[A30]}$$

(c) *Evaluation of* $\hat{\tau}_I$ *and* $\hat{\tau}_B$

The interfacial shear stress can be expressed as

$$\tau_i = \tfrac{1}{2}\rho_g f_i (U_A - C_R)^2. \qquad \text{[A31]}$$

Hence

$$\frac{\hat{\tau}_i}{\bar{\tau}_i} = 2\frac{\hat{U}_A}{\bar{U}_A - C_R} + \frac{\hat{f}_i}{\bar{f}_i}. \qquad \text{[A32]}$$

Noting that

$$\frac{\hat{f}_i}{\bar{f}_i} = \frac{\partial \bar{f}_i}{\partial \overline{\mathrm{Re}}_L}\frac{\hat{\mathrm{Re}}_L}{\bar{f}_i} \qquad \text{[A33]}$$

and using [A16] and [A28]

$$\frac{\hat{\tau}_{iR}}{\bar{\tau}_i} = 2\frac{\hat{A}_L}{A - \bar{A}_L} + \frac{\partial \bar{f}_i}{\partial \overline{\mathrm{Re}}_L}\frac{\overline{\mathrm{Re}}_L}{\bar{f}_i}\left(\frac{C_R}{\bar{u}_A}\frac{\hat{A}_L}{\bar{A}_L} - \frac{\hat{S}_L}{\bar{S}_L}\right) \qquad \text{[A34]}$$

and

$$\frac{\hat{\tau}_{iI}}{\bar{\tau}_i} = 0. \qquad [A35]$$

The amplitude term $\hat{\tau}_B$ is obtained in a manner similar to [26] and [27]. In this case, however, the gas Reynolds number, Re_G, and the hydraulic diameter, D_G, are defined differently:

$$D_G = \frac{4A_G}{(S_G + S_i)} \qquad [A36]$$

$$\mathrm{Re}_G = \frac{D_G U_A}{\nu_G}. \qquad [A37]$$

Hence

$$\frac{\hat{D}_G}{\bar{D}_G} = \frac{\hat{A}_G}{\bar{A}_G} - \frac{(\hat{S}_G + \hat{S}_i)}{(\bar{S}_G + \bar{S}_i)} \qquad [A38]$$

and

$$\widehat{\mathrm{Re}}_G = \overline{\mathrm{Re}}_G\left(\frac{\hat{U}_A}{\bar{U}_A} + \frac{\hat{D}_G}{\bar{D}_G}\right). \qquad [A39]$$

At neutral stability

$$\frac{\hat{\tau}_{BR}}{\bar{\tau}_B} \simeq 2\frac{\hat{A}_L}{A - \bar{A}_L} - \frac{\overline{\mathrm{Re}}_G}{\bar{f}_B}\frac{\mathrm{d}\bar{f}_B}{\mathrm{d}\overline{\mathrm{Re}}_G}\frac{\hat{S}_G + \hat{S}_i}{\bar{S}_G + \bar{S}_i} = 2\frac{\hat{A}_L}{A - \bar{A}_L} + \frac{1}{4}\frac{\hat{S}_G + \hat{S}_i}{\bar{S}_G + \bar{S}_i}, \qquad [A40]$$

$$\frac{\hat{\tau}_{BI}}{\bar{\tau}_B} = 0. \qquad [A41]$$

(d) *Conditions for neutral stability*

The neutral stability equations for pipe flow are reduced to algebraic equations for the simple case considered, plug flows in the gas and liquid. The substitution of [A20], [A29], [A34], [A40] into [A18] gives

$$\frac{C_R}{\bar{u}_A} = \frac{\mathrm{Num}}{\mathrm{Den}}, \qquad [A42]$$

with

$$\begin{aligned}
\mathrm{Num} = {} & 2\,\bar{\tilde{S}}_L\frac{\hat{\tilde{A}}_L}{\bar{\tilde{A}}_L} + \bar{\tilde{S}}_L\psi_L\frac{\hat{\tilde{S}}_L}{\bar{\tilde{S}}_L} + \left(1 + \frac{\bar{\tilde{A}}_L}{\bar{\tilde{A}}_G}\right)\bar{S}_i\,\bar{\tau}_i^{+}\left(2\frac{\hat{\tilde{A}}_L}{\bar{\tilde{A}}_G} - \psi\frac{\hat{\tilde{S}}_L}{\bar{\tilde{S}}_L}\right)\\
& + \bar{\tilde{S}}_G\frac{\bar{\tilde{A}}_L}{\bar{\tilde{A}}_G}\phi\bar{\tau}_i^{+}\left(2\frac{\hat{\tilde{A}}_L}{\bar{\tilde{A}}_G} + \frac{1}{4}\frac{\hat{\tilde{S}}_G + \hat{\tilde{S}}_i}{\bar{\tilde{S}}_G + \bar{\tilde{S}}_i}\right) + \left(1 + \frac{\bar{\tilde{A}}_L}{\bar{\tilde{A}}_G}\right)\bar{\tau}_i^{+}\,\hat{\tilde{S}}_i\\
& - \left(1 + \phi\,\bar{\tau}_i^{+}\frac{\bar{\tilde{A}}_L}{\bar{\tilde{A}}_G}\right)\hat{\tilde{S}}_L + (\bar{\tilde{S}}_L - \bar{\tau}_i^{+}\,\bar{\tilde{S}}_i)\frac{\hat{\tilde{A}}_L}{\bar{\tilde{A}}_L} + \left(\frac{\bar{\tilde{A}}_L}{\bar{\tilde{A}}_G}\right)^2(\phi\,\bar{\tilde{S}}_G + \bar{\tilde{S}}_i)\,\bar{\tau}_i^{+}\left(\frac{\hat{\tilde{A}}_L}{\bar{\tilde{A}}_G}\right)\\
& + \frac{2}{\bar{f}_i}\frac{\bar{\tilde{A}}_L}{\bar{\tilde{A}}_G}\frac{\hat{\tilde{A}}_L}{\bar{\tilde{A}}_G}\bar{\tau}_i^{+}\frac{\mathrm{d}\bar{\tilde{A}}_L}{\mathrm{d}\tilde{x}} - \frac{2}{f_W}\frac{\mathrm{d}\hat{\tilde{A}}_L}{\mathrm{d}x}
\end{aligned} \qquad [A43]$$

$$\text{Den} = \bar{\tilde{S}}_L (2 + \psi_L) \frac{\hat{\tilde{A}}_L}{\bar{\tilde{A}}_L} - \left(1 + \frac{\bar{\tilde{A}}_L}{\bar{\tilde{A}}_G}\right) \bar{S}_i \bar{\tau}_i^+ \psi \frac{\hat{\tilde{A}}_L}{\bar{\tilde{A}}_L} - \frac{2}{\bar{f}_W} \frac{\mathrm{d}\hat{\tilde{A}}_L}{\mathrm{d}\tilde{x}}. \quad [A44]$$

It is noted that terms involving $\mathrm{d}A_L/\mathrm{d}x$ in [A43] and [A44] are small, so that, as an approximation, these terms can be dropped.

The dimensionless interfacial stress, $\bar{\tau}_i^+$ can be expressed in a form similar to that derived for channel flow:

$$\bar{\tau}_i^+ = \left(\frac{\rho_G}{\rho_L}\right)\left(\frac{V_{SG}}{V_{SL}}\right)^{1.75}\left(\frac{\nu_G}{\nu_L}\right)^{1/4}\left(\frac{\bar{f}_i}{\bar{f}_s}\right)\left(\frac{D_L}{D_G}\right)^{1/4}\left(\frac{A_L}{A_G}\right)^{1.75}. \quad [A45]$$

The relation for parameter ψ derived for channel flow has to be modified for pipe flows to allow for pipe geometry. It is assumed that f_i/f_s is still of the same form as [45] so that $\partial \bar{f}_i/\partial h^+ = (\bar{f}_s/h^+)(\bar{f}_i/\bar{f}_s - 1)$. Here, h^+ is defined as $h^+ = hu^*/\nu_L$ with $u^* = \sqrt{\tau_W/\rho_L}$. From this it follows that

$$\Psi = \frac{\overline{\mathrm{Re}}_L}{\bar{f}_i} \frac{\mathrm{d}\bar{f}_i}{\mathrm{d}h^+} \frac{\mathrm{d}h^+}{\mathrm{d}\overline{\mathrm{Re}}_L} = \frac{\dfrac{\mathrm{Re}_L}{\bar{f}_i}\left[\dfrac{\bar{f}_s}{h^+}\left(\dfrac{\bar{f}_i}{\bar{f}_s} - 1\right)\right]}{\dfrac{\mathrm{d}\overline{\mathrm{Re}}_L}{\mathrm{d}D_L^+}\dfrac{\mathrm{d}D_L^+}{\mathrm{d}h^+}}. \quad [A46]$$

From the definition of the hydraulic diameter, D_L, and the geometric relations [A1]–[A11],

$$\frac{\mathrm{d}D_L^+}{\mathrm{d}h^+} = \frac{\mathrm{d}\tilde{D}_L}{\mathrm{d}\tilde{h}} = \frac{2}{\bar{\tilde{S}}_i \bar{\tilde{S}}_L}\left[\bar{\tilde{S}}_i^2 - (1 - 2\bar{\tilde{h}})^2 + \frac{\bar{\tilde{S}}_i}{\bar{\tilde{S}}_L}(1 - 2\bar{\tilde{h}})\right]. \quad [A47]$$

From [A22] and [A25]

$$\mathrm{Re}_L^{1.75} = 25.28\,(D_L^+)^2. \quad [A48]$$

Equations [A46] and [A48] give

$$\Psi = 0.875 \frac{\tilde{D}_L}{\tilde{h}}\left(\frac{\mathrm{d}\tilde{D}_L}{\mathrm{d}\tilde{h}}\right)^{-1}\left(\frac{\dfrac{\bar{f}_i}{\bar{f}_s} - 1}{\dfrac{\bar{f}_i}{\bar{f}_s}}\right), \quad [A49]$$

with $\mathrm{d}\tilde{D}_L/\mathrm{d}\tilde{h}$ given by [A47].

From [A45] and [49] it follows from [A42]–[A44] that $C_R/\bar{u}_A$ is a function of $\tilde{h}, f_i/f_s$, V_{SG}, V_{SL}, θ and fluid properties, i.e. variables defined by the stratified flow model.

The conditions for neutral stability are obtained from [A17] using the relation for $C_R/\bar{u}_A$, [A42], derived from [A18]. Equation [A17] can be expressed as a function of stratified flow variables by using [A19], [A20], [A29], [A30], [A34], [A35], and [A49]:

$$\frac{V_{SL}^2}{g\,D\sin\theta}\,\Omega_P\left(\frac{\bar{\tilde{A}}^2}{\bar{\tilde{A}}_L^3}\right)\left(\frac{\hat{\tilde{A}}_L}{\hat{\tilde{h}}}\right) + \frac{\rho_G}{\rho_L}\frac{\bar{\tilde{A}}_L^2}{\bar{\tilde{A}}_G^3}\frac{\hat{\tilde{A}}_L}{\hat{\tilde{h}}}\frac{V_{SG}^2}{g\,D\sin\theta} - 1 = 0, \quad [A50]$$

with

$$\Omega_P = \left(\frac{C_R}{\bar{u}_a} - 1\right)^2. \qquad \text{[A51]}$$

The flow variables V_{SG}, V_{SL}, $\tilde{\bar{h}}$, and $d\tilde{A}_L/dx$, are related by the solution of the undisturbed stratified flow model.

For fully developed inclined plug flow, the momentum balances for the two phases are

$$-A_L\frac{\partial P}{\partial x} = (\tau_W S_L - \tau_i S_i) - \rho_L A_L g\cos\theta, \qquad \text{[A52]}$$

$$-A_G\frac{\partial P}{\partial X} = (\tau_B S_G + \tau_i S_i) - \rho_G A_G g\cos\theta, \qquad \text{[A53]}$$

Making use of the Blasius formula for f_W, [A52] and [A53] gives

$$\bar{\tau}_i^+ = \left[\frac{\tilde{S}_L}{\tilde{A}_L} - \frac{2\cos\theta}{0.0791}\left(\frac{D_L V_{SL}}{\nu_L}\right)^{1/4}\left(\frac{V_{SL}}{gD}\right)^{-2}\left(\frac{A_L}{A}\right)^2\right]\left(\frac{\phi\tilde{S}_G}{\tilde{A}_G} + \frac{\tilde{S}_i}{\tilde{A}_G} + \frac{\tilde{S}_i}{\tilde{A}_L}\right)^{-1}. \qquad \text{[A54]}$$

Eliminating $\bar{\tau}_i^+$ from [A45] and [A54] yields the solution to the stratified flow problem for fully developed inclined plug flow.

For the case of a horizontal plug flow, $\theta = 90°$, so that the superficial liquid and gas velocities, V_{SG} and V_{SL}, are related by using [A45] and [A54]:

$$V_{SL} = \Xi_p V_{SG}, \qquad \text{[A55]}$$

where

$$\Xi_p^{1.75} = \left(\frac{1}{\bar{\tau}_i^+}\right)\left[\frac{\rho_G \bar{f}_i}{\rho_L \bar{\bar{f}}_s}\left(\frac{\nu_G}{\nu_L}\right)^{1/4}\left(\frac{D_L}{D_G}\right)^{1/4}\right]\left(\frac{A_L}{A_G}\right)^{1.75}. \qquad \text{[A56]}$$

Equation [A50] and [A55] give the criterion of neutral stability in a pipe as

$$\frac{V_{SG}^2}{gD} = \left(\frac{\rho_G}{\rho_L}\frac{\tilde{A}^2}{\tilde{A}_G^3}\frac{\tilde{\tilde{A}}_L}{\tilde{\tilde{h}}} + \Xi_p^2\Omega\frac{\tilde{A}^2}{\tilde{A}_L^3}\frac{\tilde{\tilde{A}}_L}{\tilde{\tilde{h}}}\right)^{-1}. \qquad \text{[A57]}$$

It is noted that the right-hand side of [A56] is a function of $\tilde{h}$, f_i/f_s pipe diameter and fluid properties.

$$\Xi = \frac{1}{60.15}\left(\frac{1-\alpha)}{\alpha}\right)^2\left[1 + \frac{4}{3}\left(\frac{1-\alpha}{\alpha}\right)\right]\left(\frac{\rho_G}{\rho_L}\right). \qquad \text{[A58]}$$